JOURNAL OF CATALYSIS **180,** 66–84 (1998)
ARTICLE NO. CA982256

Reaction of Hexane, Cyclohexane, and Methylcyclopentane over Gallium-, Indium-, and Thallium-Promoted Sulfated Zirconia Catalysts

V. Pârvulescu,* S. Coman,† V. I. Pârvulescu,†,[1] P. Grange,‡ and G. Poncelet‡

*Institute of Physical Chemistry, Spl. Independentei 202, Bucharest 77208, Romania; †Department of Chemical Technology and Catalysis, Faculty of Chemistry, University of Bucharest, B-dul Republicii 13, Bucharest 70346, Romania; and ‡Unité de Catalyse et Chimie des Matériaux Divisés, Université Catholique de Louvain, Place Croix du Sud 2/17, 1348 Louvain-la Neuve, Belgium

Received May 15, 1998; revised August 3, 1998; accepted August 4, 1998

Sulfate–zirconia catalysts were prepared via the colloidal-sol–gel method using $ZrOCl_2$ as precursor. After precipitation and washing, the solids were peptized with a 1 : 1 mixture of CH_3COOH and H_2SO_4. The promoters were introduced as gallium, indium, or thallium nitrates into the solution containing the zirconium sols. After a gel formation period, the samples were dried and calcined. The catalysts were characterized by chemical analysis, nitrogen sorption isotherms, FTIR analysis of adsorbed pyridine and deuterated acetonitrile, XRD, laser Raman and FTIR spectroscopy, and XPS. The catalytic tests were performed in a fixed-bed quartz microreactor using as reactant molecules hexane, cyclohexane, and methylcyclopentane. Characterization of the samples by the different techniques allowed us to propose that the main factors controlling the observed properties are the high sulfur content and the promoter effect. Low surface areas of the catalysts were related to the high sulfur contents. Sulfate species in different coordinations were indentified: isolated sulfate groups, polynuclear sulfate species, and sulfuric acid. Lewis acid sites as well as the polynuclear sulfate species determined the acidity of these solids. The presence of promoters contributed not only to the increase of the redox behavior of the catalysts, but also to a decrease of the population of polynuclear sulfates, in the order Tl > In > Ga. In the reaction conditions adopted, on unpromoted catalysts and (especially) Ga-promoted catalysts, dehydroizomerization and ring isomerization were the principal reaction pathways for hexane and methylcyclopentane, and for cyclohexane, respectively. Tl was found to promote ring cleavage. These data are consistent with previous studies pointing to the dehydrogenation activity of Ga embedded in zeolite matrices.

INTRODUCTION

Some 20 years ago, sulfated oxides such as $ZrO_2 \cdot SO_4^{2-}$, $TiO_2 \cdot SO_4^{2-}$, $SnO_2 \cdot SO_4^{2-}$, $Fe_2O_3 \cdot SO_4^{2-}$, and $HfO_2 \cdot SO_4^{2-}$ (1–5) initiated a hot topic in catalysis, namely the synthesis of new solid acid catalysts for the isomerization of lower alkanes. Recently, other solid catalysts such as sulfated alumina (6) and sulfated ceria (7) have been reported. Many studies have focused on the preparation and characterization of sulfated zirconia because these catalysts were claimed to exhibit superacidic properties. However, this point of view has recently been questioned (8, 9) and now it is generally accepted that these solids are merely strong acid catalysts.

Early in the nineties, a new class of sulfated metal oxides was described by Hsu and co-workers (10–13) who showed that promotion of sulfated zirconia with Fe and Mn increased activity by nearly three orders of magnitude and that these new catalysts were able to isomerize butane at temperatures as low as near room temperature. In subsequent studies on the reaction of butane and propane, Cheung *et al.* (14, 15) concluded that promoted sulfated zirconia is a stronger acid than sulfated zirconia. Davis and co-workers (16, 17) and Srinivasan *et al.* (8) proposed that the particular activity of these catalysts was not due to the increased acidity, but instead to a modification of the electron acceptor ability of sulfated zirconia with, as a result, the enhancement of the redox properties. The first step of the reaction mechanism of butane consists in the dehydrogenation of the alkane which, in the second step, leads to the iso-alkane via a bimolecular mechanism. Lately, Ghenciu and Farcasiu (18) provided evidence for the existence of an additional radical pathway. The modification of the ZrO_2 surface by iron was further confirmed by Sikabwe and White (19). Promotion of sulfated zirconia with Ni was found by Alvarez *et al.* (20) to be less effective than with Fe and Mn. Vera *et al.* (21) compared the activity of several promoted sulfated zirconias in the isomerization of butane and showed that promotion by Fe, Co, Cr, W, Ni, or Pt gave more active systems than sulfated zirconias, whereas Cu-, Zn-, or Cd- promoted catalysts were less active.

Another attempt to improve the activity of sulfated zirconia catalysts was made by Lonyi *et al.* (22), who sulfated

[1] To whom correspondence should be addressed.

0021-9517/98 $25.00

TABLE 1

Chemical Composition and Textural Characteristics of the Investigated Samples

Sample	Promoter content wt% metal oxide	Sulfate content wt%	Activated in Ar at 550°C			Activated in air at 550°C			
			SO_4^{2-} groups · nm^{-2}	Surface area $m^2 \cdot g^{-1}$	Average pore diameter, Å	Sulfate content wt%	SO_4^{2-} groups · nm^{-2}	Suface area $m^2 \cdot g^{-1}$	Average pore diameter, Å
$ZrO_2 \cdot SO_4^{2-}$	—	19.3	16.3	84	48	18.3	17.4	76	42
$ZrO_2 \cdot Ga_2O_3 \cdot SO_4^{2-}$	15.0	18.2	18.1	78	49	14.2	14.6	71	40
$ZrO_2 \cdot In_2O_3 \cdot SO_4^{2-}$	15.1	18.4	26.1	75	45	11.4	12.4	68	40
$ZrO_2 \cdot Tl_2O \cdot SO_4^{2-}$	15.0	18.1	2.71	48	62	5.8	2.5	45	60

a mixture of titania–zirconia oxides, but in this case the promoting effect was unclear.

All these studies came to the conclusion that the reaction of hydrocarbons with less than five carbon atoms occurs via a bimolecular mechanism (23), while for those with more than five carbon atoms, a monomolecular mechanism would be involved (24, 25). In both cases, however, the dehydrogenating function of the catalysts appears to be very important.

These results were the starting point of this study. In the aromaticisation of lower alkanes, it has been proved that the insertion of Ga in the ZSM-5 structure had a promoting effect on the dehydrogenation activity (26–31). Attempts at using In or Tl were also reported (32) but the results were not as convincing. With this background, our study aimed to investigate the effect of promoting $ZrO_2 \cdot SO_4^{2-}$ with Ga, In, or Tl in the reaction of C_6 hydrocarbons, namely hexane, cyclohexane, and methylcyclopentane. The reaction of these hydrocarbons over sulfated zirconia catalysts was previously reported in the literature (22, 33–36). The characterisation of the structures resulting from the promotion with Ga, In, or Tl was another target of the present investigation.

METHODS

2.1. Catalysts Preparation

The catalysts were prepared via the colloidal-sol–gel method. Briefly, 90 mmol $ZrOCl_2 \cdot 6H_2O$ were dissolved in water and precipitated with NH_3 solution (18 wt%) at pH = 9.0. The precipitate was washed free of Cl^- with distilled water and then peptized with a 1 *M* solution of a 1 : 1 mixture of CH_3COOH and H_2SO_4. Peptization was completed after 6 h. To the solution containing zirconium sols, 0.12 *M* solution of either gallium, indium, or thallium nitrate was added. Gelification was carried out at 60°C for 3 weeks. The samples were dried overnight under vacuum and then calcined at 550°C for 6 h in argon flow for the one part, or in air flow for the other part, using a ramp of 0.14°C min^{-1}. The chemical composition of the samples was determined by inductively coupled plasma atomic emission spectrometry (ICP-AES) and the results are given in Table 1.

2.2. Catalysts Characterization

Samples were characterized by N_2 sorption at 77 K, FTIR analysis of adsorbed pyridine and deuterated acetonitrile, XRD, laser Raman and laser FTIR spectroscopy, and XPS. The nitrogen sorption isotherms at 77 K were obtained in an ASAP 2010 sorptometer from Micromeritics, after outgassing the samples at 200°C for 12 h.

The surface acidity was characterized by IR spectroscopy of adsorbed pyridine (Py) and deuterated acetonitrile (DA) (both with Aldrich purity). The spectra were recorded with a Nicolet 60SX spectrometer, with a resolution of 2 cm^{-1}. Prior to adsorption of the bases, the powder samples were calcined at 550°C for 2 h under an air flow of 30 ml min^{-1}. Self-supporting wafers obtained by compression (about 12 mg cm^{-2}) were outgassed in the IR cell at 400°C at a residual pressure of 0.1 mPa. After adsorption of the probes, the samples were purged for 2 h with He at 150°C to remove the weakly sorbed species.

XRD analysis of the samples was made with a SIEMENS D-5000 diffractometer powered at 40 kV–50 mA, and equipped with a variable-slit diffracted-beam monochromator and scintillation counter. The diffractograms were recorded in the range 0–80° 2θ at a scanning speed of 0.5° 2θ min^{-1} using Cu$K\alpha$ radiation ($\lambda = 1.5418$ Å).

The Raman spectra were recorded on a Dilor–Jobin Yvon-SPEX spectrometer equipped with an optical multichannel analyzer. The Raman spectra were excited with the 488-nm line of an Ar^+-ion laser. Self-supporting wafers were prepared from powder samples preactivated for 6 h at 550°C in Ar or in air.

The XPS spectra were recorded using a SSI X probe FISONS spectrometer (SSX-100/206) with monochromated Al$K\alpha$ radiation. The spectrometer energy scale was calibrated using the Au $4f_{7/2}$ peak (binding energy 84.0 eV). For the calculation of the binding energies, the C 1*s* peak of the C–(C,H) component at 284.8 was used as an

internal standard. The composite peaks were decomposed by a fitting routine included in the ESCA 8,3 D software.

2.3. Catalytic Tests

Catalytic tests were performed in vapour phase, in a fixed-bed quartz microreactor operated at atmospheric pressure using 0.4 g catalyst (calcined *in situ* in the conditions mentioned earlier), and as reactants hexane, cyclohexane, and methylcyclopentane (all from Merck). The hydrocarbon/Ar (1 : 1 ratio) gas mixture was preheated at 120°C and then passed over the catalyst bed at space velocity of 5.4 h^{-1}. The experiments were carried out in the temperature range 120–240°C. One-line analysis of the gaseous effluent was made in a gas Pye-Unicam 104 chromatograph. The reaction rates were determined by extrapolating the declining conversions to zero time on stream. The apparent activation energies were obtained from the Arrhenius plots. TOF was calculated as mmol hydrocarbon reacted/mmol sulfate/s.

RESULTS

3.1. Textural Characteristics

Figures 1 and 2 show the N_2 adsorption–desorption isotherms of the samples activated in argon and air, respectively. The hystereses were of type II for the samples activated in Ar, except for the Tl-containing sample, which was of type III. According to Sing and Rouquerol (37), such a hysteresis indicates a porous structure in which the adsorbent does not possess a well-defined mesopore structure. The pore size distribution calculated from the desorption branch (BJH method) was quite narrow for $ZrO_2 \cdot SO_4^{2-}$ as well as for the samples containing Ga or In, whereas for the Tl-promoted sample, a second maximum corresponding to pores with 65-Å diameter was observed. The values are given in the Table 1 together with the BET specific surface areas. It is noticeable that all the BET surface areas were almost identical to those calculated by the *t*-plot method, confirming the absence of a microporous texture. The Tl-containing sample exhibited lower BET surface area and greater pores than the other samples.

Air activation gave solids with lower BET surface areas than those activated in Ar. Near type III hystereses were obtained for all the samples (Fig. 2). The textural characteristics of the samples activated in air are given in Table 1.

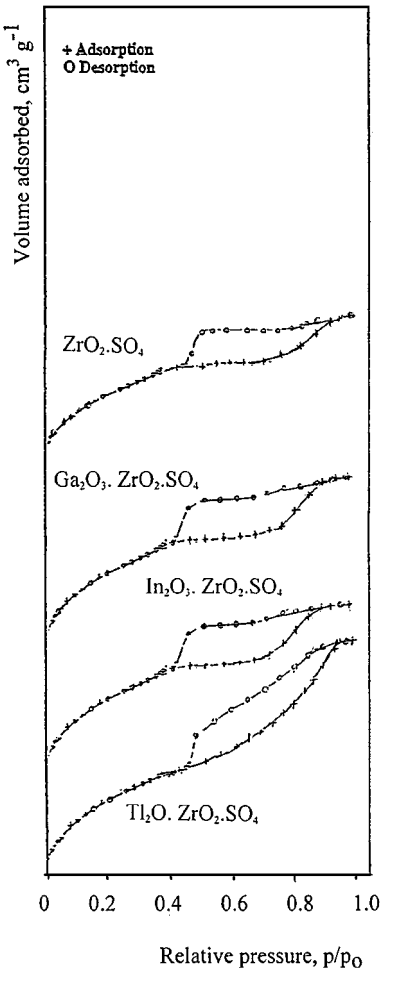

FIG. 1. Nitrogen adsorption–desorption isotherms of samples activated in argon flow.

3.2. Measurements of Acidity by FT-IR Spectroscopy of Adsorbed Probe Molecules

3.2.1. FT-IR Spectra of Adsorbed Pyridine

Figure 3 shows the FT-IR spectra recorded at room temperature in the region 1400–1700 cm^{-1}, after adsorption of Py on the different sulfated-zirconia samples activated in Ar (solid line) and in air (dotted line), respectively.

The spectra show the typical Py-IR absorption bands of such materials (38–41) assigned to the 8a and 19b vibration modes of adsorbed-Py forming Lewis-type adducts (Py-L with bands at 1610 and 1448 cm^{-1}), and to the 8a and 19b modes of Py in interaction with Brønsted acid sites (Py-B with bands at 1640 and 1542 cm^{-1}). The intensity of these bands changes from one catalyst to the next one, according to the chemical composition and atmosphere in which these samples were activated. The two other bands at 1577 and 1490 cm^{-1} are assigned to Py adsorbed on either Lewis or Brønsted acid sites.

A closer examination of these spectra shows several features. For the samples activated in Ar (solid line) at 550°C:

(i) The intensity of the band at around 1610 cm^{-1} increases going from the bottom spectrum (sample containing Tl) to the top spectrum (sample without promoter). It seems that the replacement of Tl by Ga or In, and particularly the absence of promoter, leads to an enhancement

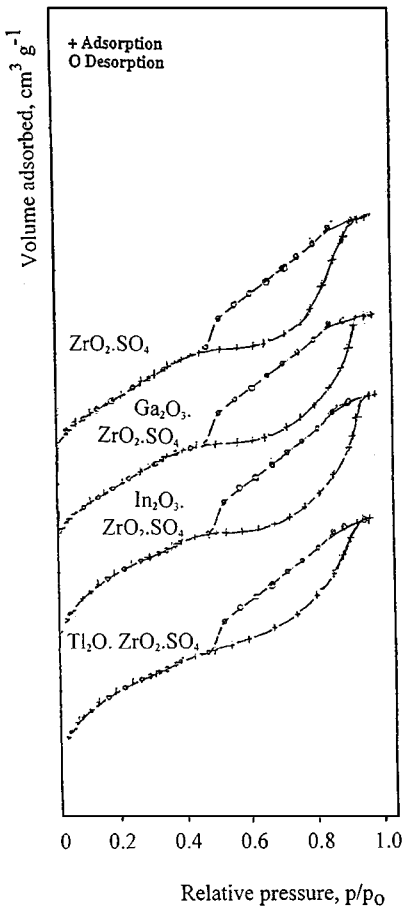

FIG. 2. Nitrogen adsorption–desorption isotherms of samples activated in air flow.

of the acidity of the surface Lewis acid sites. Such a behavior, according to Morterra *et al.* (42), could also be associated with the formation of polynuclear sulfates which is precluded by the presence of Tl. The second band, due to Py adsorbed on Lewis acid sites (1448 cm^{-1}), follows similar behavior with the modification of the chemical composition.

(ii) The intensity of the band at 1542 cm^{-1} is also sensitive to the chemical composition. The population of Brønsted acidic sites is higher in the nonpromoted sample than in the promoted ones. A similar observation was previously reported by Nascimento *et al.* (43) for increasing sulfur contents. Indeed, these authors also observed a shift in the band position with the modification of the sulfur content. This could be another indication that the presence of promoters, and mainly Tl, inhibits the formation of some complex sulfates which exhibit Brønsted acidity.

(iii) Generally, the band located around 1490 cm^{-1} is not discussed in the literature because it characterizes Py interacting with both Lewis and Brønsted acid sites. However, the variation of this band shows that promotion produces an increase of the sum of both kinds of acid sites.

Activation of the same samples in air at 550°C has the following effects:

(i) In the case of the Lewis acid sites, air activation leads to a very small shift (3–4 cm^{-1}) to higher wavenumbers of both bands assigned to adsorbed Py species, irrespective of the nature of the promotor. Also, a reduction of the band intensities is noticed, which may suggest that air activation facilitates the interaction of sulfate and of polysulfate groups with the ZrO_2 carrier with, as a result, a decrease of the amount of the Brønsted sites and a small increase of the strength of the Lewis sites.

One should note that for the air-activated samples, the band assigned to Py-L is located at slightly higher

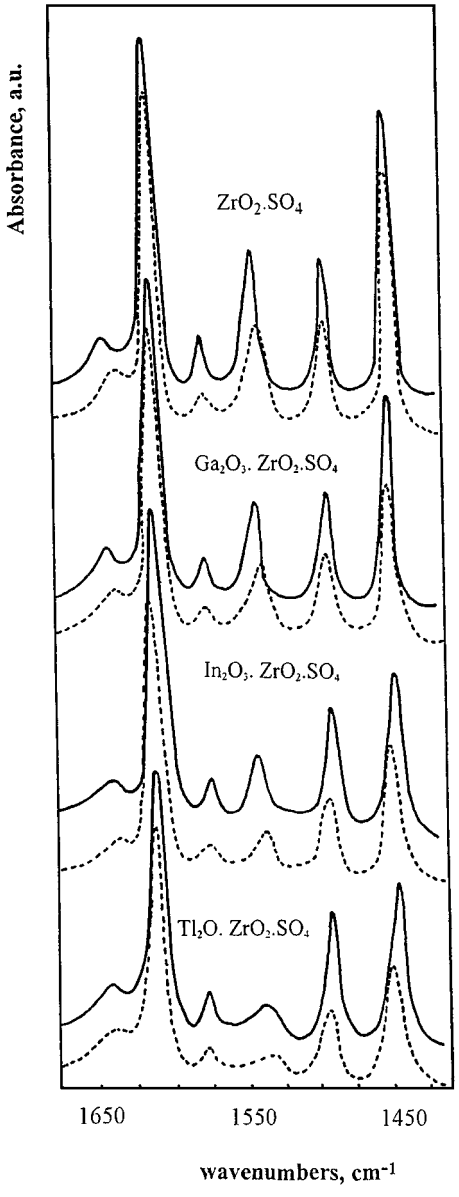

FIG. 3. FT-IR spectra of Py adsorbed on the different sulfated-zirconia samples activated in Ar (solid line) and in air (dotted line).

wavenumbers compared with the spectra recorded for samples activated in argon. The presence of promoters produces a shift to lower wavenumbers.

(ii) For the promoted samples, a relatively more pronounced decrease of the band intensity is observed for the bands assigned to Py adsorbed on Brønsted acid sites. But in this case, the shift occurs in the opposite direction, i.e., to lower wavenumbers. This behavior could indicate that there is, indeed, a direct relation between the strength of Brønsted acid sites and the promoting species.

3.2.2. FT-IR Spectra of Deuterated Acetonitrile

Figure 4 shows room temperature FT-IR spectra in the region 2200–3800 cm^{-1} of CD_3CN adsorbed on the different sulfated samples activated in Ar (solid line) and in air (dotted line). The spectra show broad absorptions between 3650 and 2800 cm^{-1} indicating an interaction of CD_3CN with acidic protons present at the surface of the samples. The other band at 2305 cm^{-1}, according to van Santen and co-workers (44, 45), corresponds to the C–N stretching frequency of CN bonded either to Brønsted or to Lewis acid sites. The other two bands at 2250 and 2112 cm^{-1} are due to the C–D stretching modes.

The examination of the spectra of Fig. 4 provides information complementing those obtained from FT-IR of adsorbed Py:

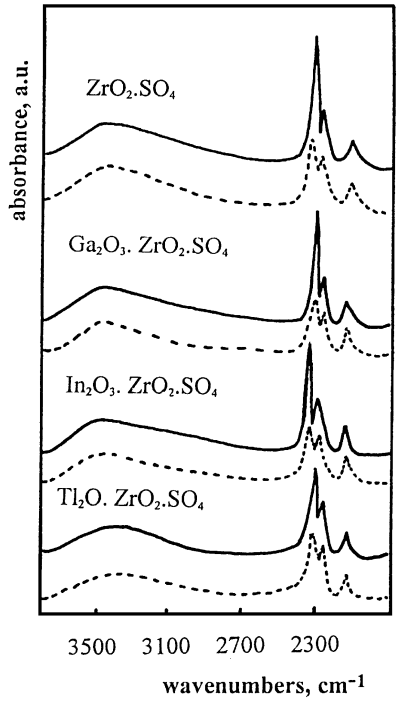

FIG. 4. FT-IR spectra of adsorbed CD_3CN on the different sulfated zirconia samples activated in Ar (solid line) and in air (dotted line).

(i) The intensity of the band at around 2305 cm^{-1} decreases in the order $ZrO_2 \cdot SO_4^{2-} > ZrO_2 \cdot Ga_2O_3 \cdot SO_4^{2-} > ZrO_2 \cdot In_2O_3 \cdot SO_4^{2-} > ZrO_2 \cdot Tl_2O \cdot SO_4^{2-}$. This decrease, together with a simultaneous shift of the band by about 10 cm^{-1} to lower wavenumbers, suggests that promotion results in a lowering of the total amount of the acid sites (Brønsted and Lewis) and of the average acid strength.

(ii) The interaction of the basic CN with acidic protons present in sulfated oxides shifts the OH band to lower wavenumbers and causes band broadening. The area of this broad band is also related to the promoter element.

(iii) Activation in air produces a small decrease in the intensity of the broad band between 3650 and 2800 cm^{-1} and of the one near 2305 cm^{-1}. However, no clear shift of these bands was noticed compared with the spectra recorded for samples activated in Ar, perhaps indicating some compensation effect between the two types of acid sites (Brønsted and Lewis).

3.3. Structural Characterization

3.3.1. Raman Spectra

Raman spectra recorded for samples activated in Ar and air are presented in Figs. 5 and 6, respectively. The spectra show some clear differences and, therefore, they will be discussed separately. There is already a good agreement in the literature on the band assignment (46–48).

3.3.1.1. Samples activated in Ar. Samples activated in Ar exhibit bands which are attributed to S–O and S=O stretching modes of the sulfate group, at 1017 and 1040 cm^{-1}, and at 1390 cm^{-1}, respectively. According to Babou *et al.* (40, 49), the band at 1017 cm^{-1} corresponds to S–O stretching modes in isolated SO_4^{2-} species, and the one at 1040 cm^{-1}, to adsorbed (H_2SO_4) species. The band located between 1117 and 1127 cm^{-1} is assigned to S–O stretching modes in bidentate sulfate species (40, 49). The bands in the low frequency region (<700 cm^{-1}) are mainly due to zirconia. Recordings of pure tetragonal and monoclinic phases allowed us to assign the bands in this region to these two phases (Fig. 5). No band that could be assigned to Ga, In, or Tl oxide was found.

Summarizing, the samples activated in Ar contain both tetragonal and monoclinic phases, and the sulfate groups in these catalysts coexist both as isolated and bidentate species, as well as deprotonated SO_4^{2-} groups and H_2SO_4 adsorbed species. The differences in the relative intensity of the bands are in direct dependence on the type of promoter.

3.3.1.2. Samples activated in air. Samples activated in air exhibit bands in the region of the S–O and S=O stretching modes, except for a new one, located at 1060 cm^{-1} (Fig. 6). According to Babou *et al.* (40, 49), this band can also be attributed to S–O stretching modes but in polynucleated sulfate groups. Its presence indicates that calcination in air

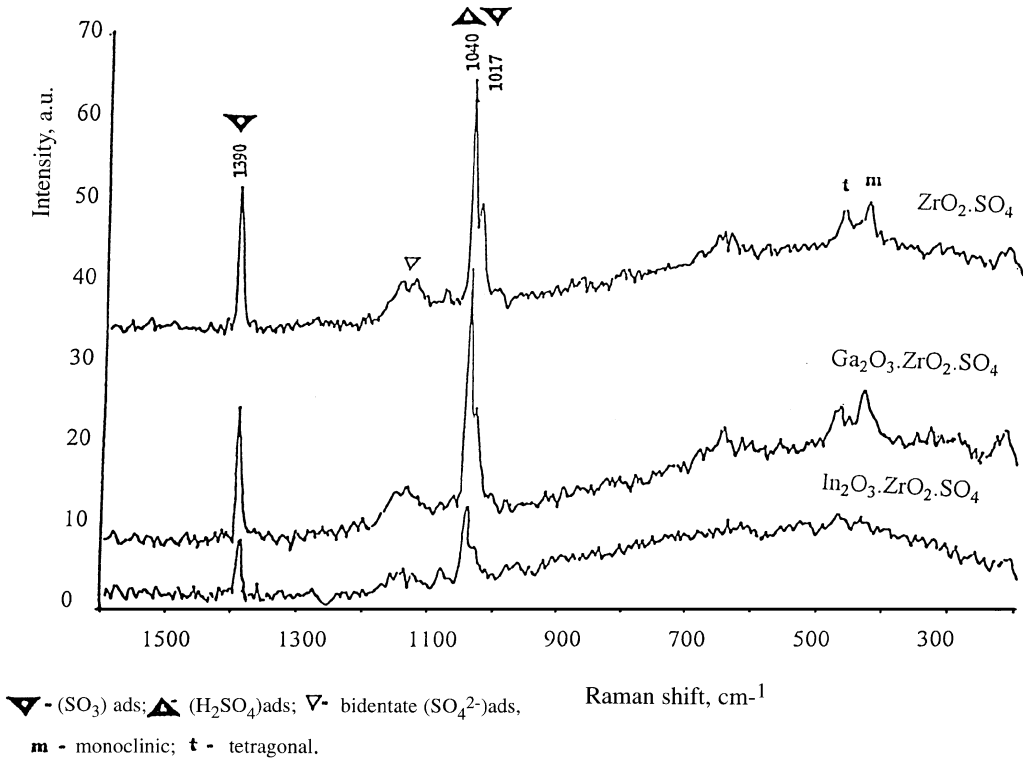

FIG. 5. Raman spectra recorded for samples activated in Ar at 550°C.

facilitates the condensation of sulfate species to polynucleated ones. It is interesting to note that the bands near 1117 cm^{-1} are better defined in the Ga-promoted and for the unpromoted samples. In the low-frequency region, only the Raman bands attributed to the monoclinic phase are observed.

It appears that activation in air leads to a more heterogeneous surface in which the population of the nucleated

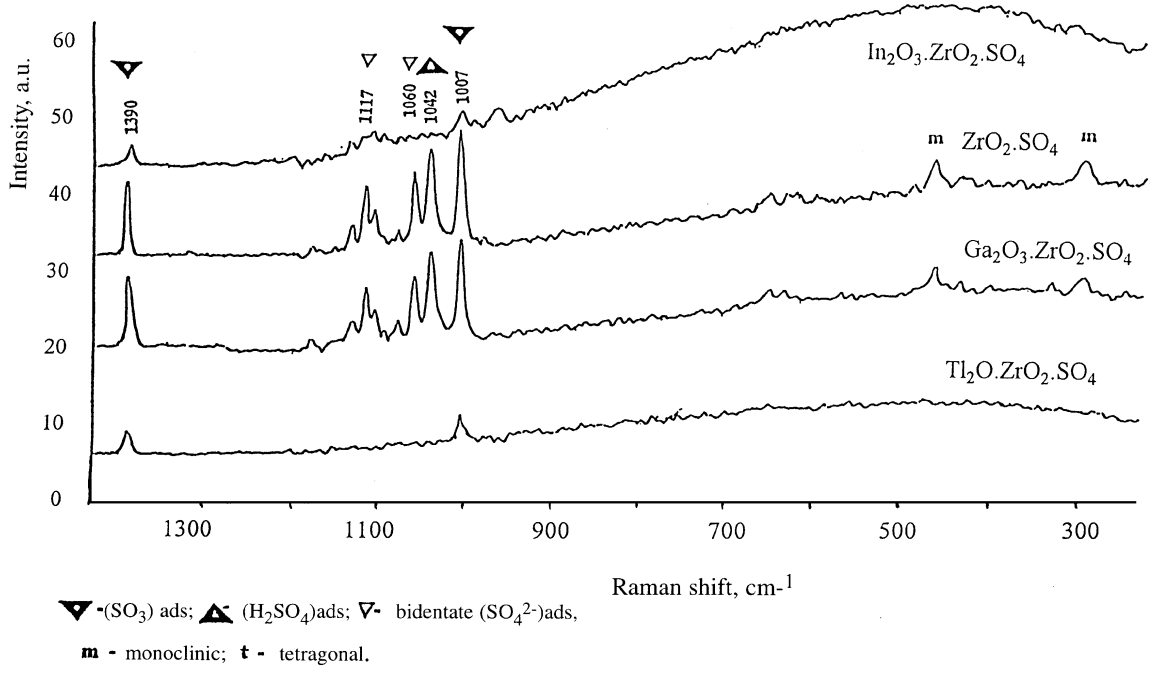

FIG. 6. Raman spectra recorded for samples activated in air at 550°C.

sulfate species is increased as in the case of the samples activated in Ar. The differences among the investigated samples appear in the relative intensity of the bands which are directly related to the sulfur content.

3.3.1.2. Samples exposed to hydrocarbon vapour. Wafers of unpromoted and promoted catalysts (previously calcined in air and in Ar in the conditions indicated earlier) were exposed for 1 h at 140°C to hexane, methylcyclopentane, and cyclohexane, and the Raman spectra were recorded after the cells were outgassed. Only the results obtained for the Ga-promoted systems will be discussed.

The spectra of the samples activated in air and in Ar atmosphere and then exposed to the different hydrocarbons are shown in Figs. 7 and 8, respectively. The spectra of the samples treated with hexane and cyclohexane exhibit similar features for both air- and Ar-activated samples. The S–O stretching modes assigned to isolated deprotonated sulfate groups (at 1017 cm^{-1}) are absent, while well-defined S–O and S=O stretching bands of adsorbed H_2SO_4 at 1040 and 1391 cm^{-1} are observed, the latter probably overlapping with other species. It is also worth noting that no bidentate (or polysulfate) species are present (band at 1117 cm^{-1}). Concomitant with the modifications occurring in the sulfate coordination, the spectra show that the structure of zirconium oxide is also modified. Indeed, after activation both in Ar and in air, bands due to the tetragonal phase show up (bands at 588, 514, and 217 cm^{-1}).

The organic contaminants give rise to different absorptions. A band attributed to polyenic cations is observed at 429–433 cm^{-1}. Also, an intense band at 1500–1517 cm^{-1} is assigned to C=C stretching vibrations. This band was relatively more intense for the sample treated with cyclohexane than with hexane, again independent of the activation atmosphere. According to Spielbauer *et al.* (47), the frequency of this band indicates a more or less pronounced aromatic character. It was also found that the intensity of this band increased in the sequence $ZrO_2 \cdot Ga_2O_3 \cdot SO_4^{2-} > ZrO_2 \cdot SO_4^{2-} > ZrO_2 \cdot In_2O_3 \cdot SO_4^{2-} > ZrO_2 \cdot Tl_2O \cdot SO_4^{2-}$.

The spectra recorded on samples exposed to methylcyclopentane differ from those recorded for either hexane or cyclohexane. The band at 1517 cm^{-1} is completely absent.

Clear differences are noted in the region of the sulfate bands as a function of the calcination atmosphere and of the nature of the organic molecule the samples were exposed to. The spectra recorded for the sample activated in Ar still show the band at 1019 cm^{-1} due to nonprotonated isolated SO_4^{2-} groups. For the samples activated in air, this band disappears but three components are clearly defined in the region 1385–1430 cm^{-1}. In agreement with several authors (7, 41, 50, 51), the band located at 1423 cm^{-1} could be assigned to S=O stretching modes in disulfate species.

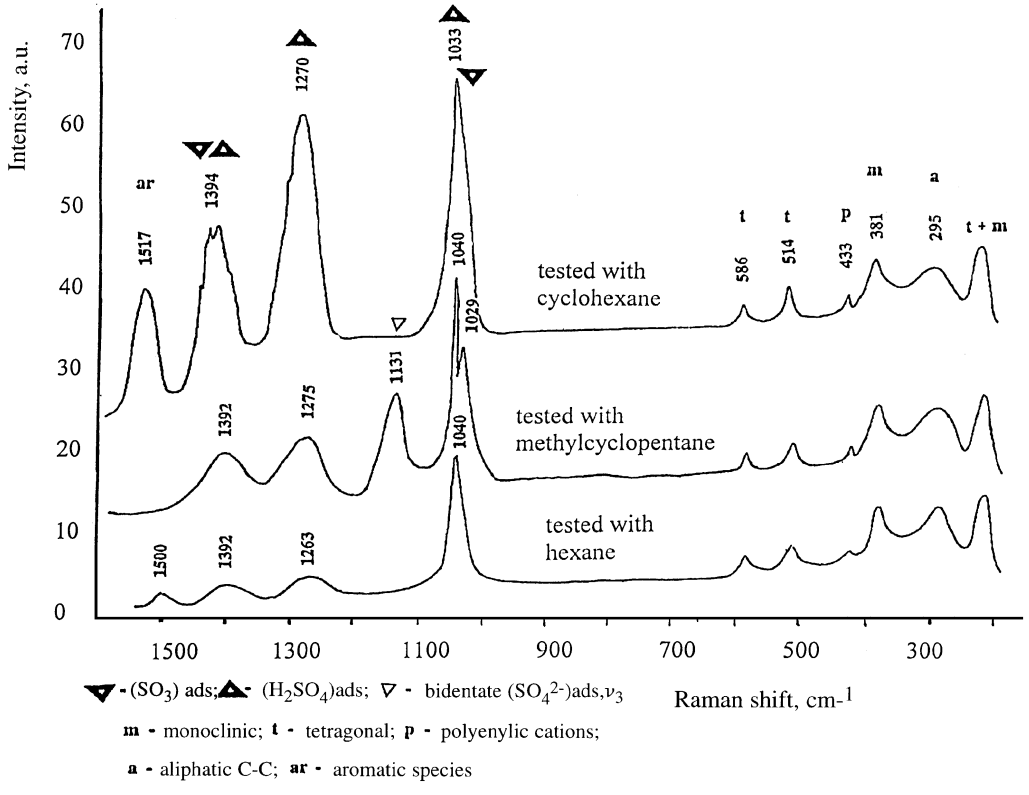

FIG. 7. Raman spectra of Ga-promoted sulfated zirconia activated in Ar, after exposure to hydrocarbons.

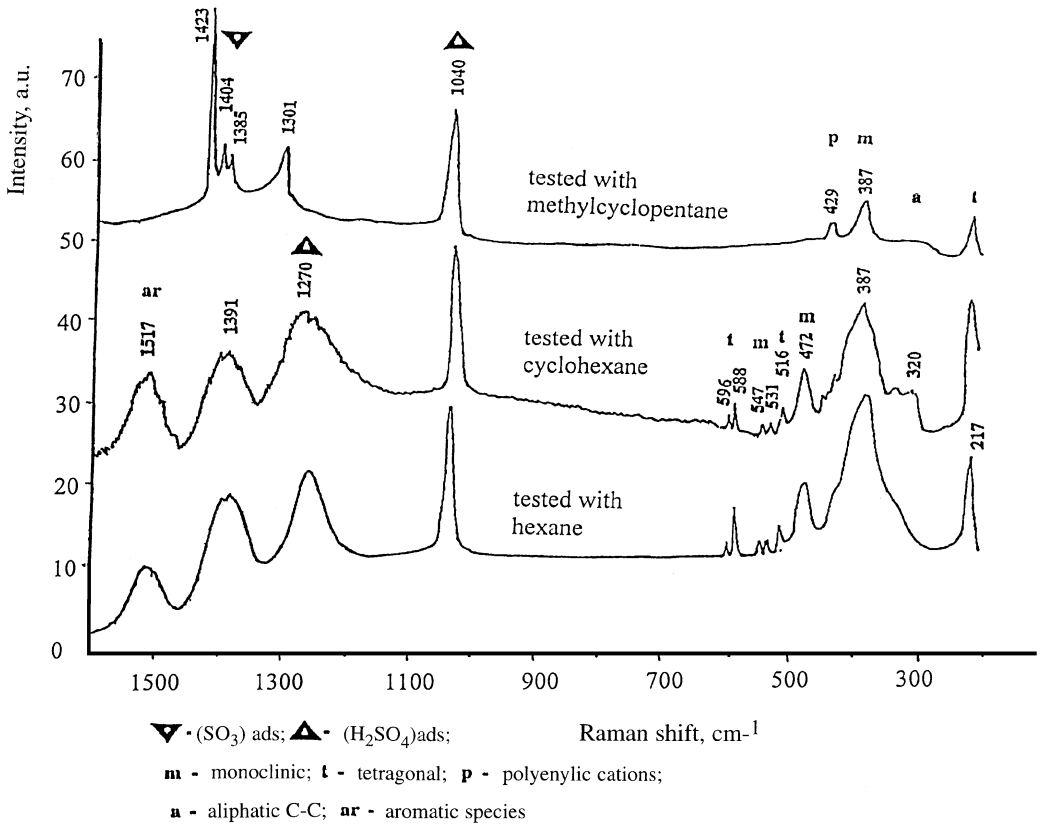

FIG. 8. Raman spectra of Ga-promoted sulfated zirconia activated in air, after exposure to hydrocarbons.

According also with the literature data (5, 7), the bands at 1404, 1385, and 1131 cm^{-1} are assigned to surface polydentate sulfate species whereas that at 1131 cm^{-1} to bulk-like species. It is worth mentioning that the decomposition of the band centered at 1391–1394 cm^{-1} in the spectra recorded after exposure to hexane and cyclohexane shows that this band is also present. But, according to the model proposed by Bensitel *et al.* (50), which is now generally accepted, it is difficult to explain why the stretching S–O modes disappeared while the stretching S=O modes became more evident. Another assignement for this band could be the one proposed by Spielbauer *et al.* (47), who attributed a band at 1450 cm^{-1} to increased aromatic character of the organic contaminants. But in our case, the shape of the band as well as the missing band at 1517 cm^{-1}, which should also show up for such species, does not support this assignment. In addition, Ga was found to have no influence on this species. Therefore, we suppose that, taking into account also the high amount of sulfate in the investigated samples, different monosulfate species co-exist and at least one of those could correspond to protonated species.

3.3.2. XRD Analysis

The X-ray patterns of the sulfated oxide samples activated in Ar and in air are shown in Figs. 9 and 10, respectively. All the Ar-activated samples contain crystalline phases corresponding to two different types of zirconium sulfate (ASTM 24-1492 and ASTM 24-1498) and to tetragonal ZrO_2 (ASTM 34-1484). In addition, peaks corresponding to ZrOS (ASTM 4-0897) and to an unknown phase (indicated by ? in the figures) were also found. No line corresponding to Ga, In, or Tl compounds could be evidenced.

Activation in air leads to more crystalline structures. The same crystallographic phases were identified, except for ZrOS, but the number of diffracting planes was much increased. In addition, instead of tetragonal ZrO_2, only the lines corresponding to monoclinic ZrO_2 (ASTM 34-1484) were observed. The complexity of the patterns of the promoted samples and the apparent peak splittings require a more detailed crytallographic analysis which will be addressed in further work. Perhaps the phases in presence could be mixtures of zirconium sulfate and promoter-containing zirconium sulfate.

In conclusion, activation in air produces a far more complex mixture of crystalline sulfate phases compared to activation in argon.

3.3.3. XPS Spectra

The XPS data are given in the Table 2, and typical XPS spectra in the region of S_{2p} are illustrated in Fig. 11. The data of Table 2 allow us to stress several points.

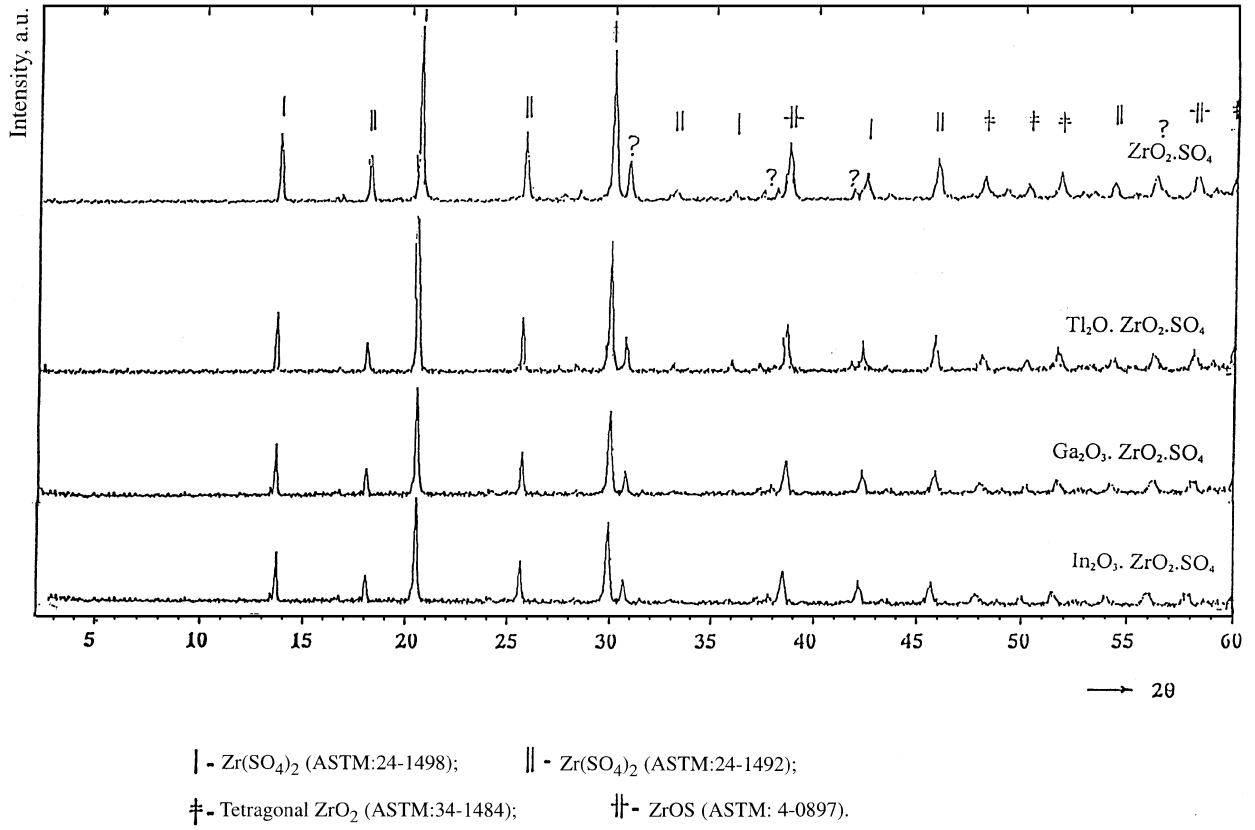

FIG. 9. X-ray diffraction patterns of sulfated zirconia samples activated in Ar.

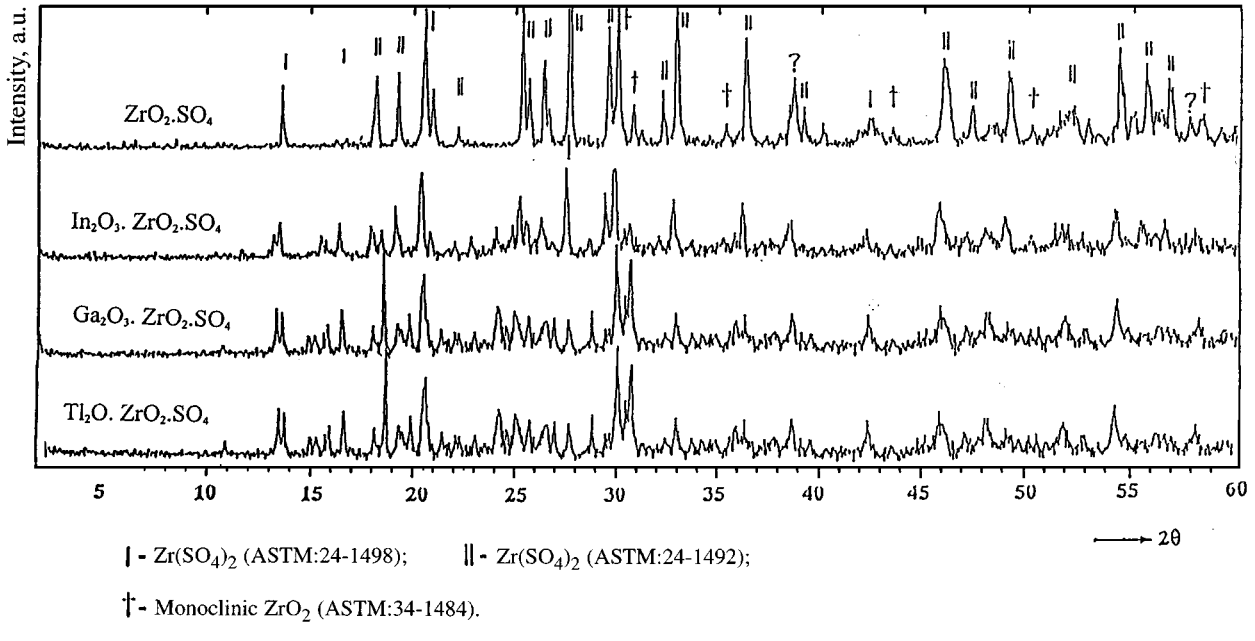

FIG. 10. X-ray diffraction patterns of sulfated zirconia samples activated in air.

TABLE 2

XPS Parameters of the Investigated Catalysts

Species	$ZrO_2 \cdot SO_4^{2-}$		$ZrO_2 \cdot Ga_2O_3 \cdot SO_4^{2-}$		$ZrO_2 \cdot In_2O_3 \cdot SO_4^{2-}$		$ZrO_2 \cdot Tl_2O \cdot SO_4^{2-}$	
	Treated in Ar 550°C	Treated in Air 550°C	Treated in Ar 550°C	Treated in Air 550°C	Treated in Ar 550°C	Treated in Air 550°C	Treated in Ar 550°C	Treated in Air 550°C
S 2*p*	168.9	169.1	169.1	169.4	168.7	169.1	168.5	169.1
S 2*p*	170.2	170.4	170.4	170.7	170.0	170.4	169.8	170.4
Zr 3*d*5	184.2	184.2	183.9	183.8	184.1	184.0	184.6	184.5
Zr 3*d*3	186.6	186.6	186.3	186.2	186.5	186.4	187.0	186.9
S/Zr	2.31	1.92	2.32	1.94	2.60	2.15	2.66	2.18
S/(Zr + *M*)	—	—	1.97	1.64	1.90	1.57	1.88	1.54
S_{169}/S_{170}	1.26	1.69	1.65	1.89	1.25	1.38	1.17	1.25
Ga 3*s*	—	—	162.1	162.2	—	—	—	—
Ga 3*d*	—	—	21.4	21.5	—	—	—	—
In 3*d*5	—	—	—	—	445.8	446.0	—	—
In 3*d*3	—	—	—	—	453.4	453.6	—	—
Tl 4*f*7	—	—	—	—	—	—	120.7	120.9
Tl 4*f*5	—	—	—	—	—	—	125.2	125.4

(i) *State of zirconium*. The values determined for zirconium are in a rather large range of binding energies and correspond to Zr in the oxidation state (IV) (52). Promotion with Ga seems to generate more "acidic" zirconium species compared with nonpromoted sulfated zirconia. Promotion with Tl has an opposite effect, whereas In has almost no effect. The same shift was observed both for the Zr $3d_5$ and Zr $3d_3$ binding energies. Air activation seems to have no influence on the oxidation state of Zr compared with samples activated in Ar.

(ii) *State of sulfur*. The binding energies of sulfur were recorded in the region corresponding to the 2*p* energies. As shown in Fig. 11, the peak corresponding to these species exhibits a pronounced asymmetry. Decomposition of this peak using the machine routine leads to two components, the one with BE at around 169 eV and the other one at around 170 eV. The correlation of the change of the ratio of these species with those determined from FT-IR measurements (Py) and Raman allows one to propose that the first component (at around 169 eV) corresponds to deprotonated sulfate species, and the one near 170 eV, to protonated species. The high ratio for the sample promoted with Ga compared with the non-promoted sample indicates the predominance of deprotonated sulfated species. Promotion with In seems to have no effect on the sulfur state, while for Tl, there is a tendency to a slight increase of the population of protonated species.

The presence of promoters also results in a tendency to shift the binding energies from lower values (Tl) to higher values (Ga), which could indicate a more advanced interaction of the sulfate groups with the zirconium oxide support. The atmosphere in which the samples were activated also brought about some modifications in the position and shape of the S 2p peak. Indeed, calcination in air also tends to shift the binding energy to higher values, which could be caused by the same interaction of sulfate groups with the support. At the same time, air activation provokes an increase of the proportion of sulfur atoms belonging to the S_{2p} component with binding energy of 169, which may also reflect an increase of the population of deprotonated sulfate species.

(iii) *Sulfur-to-metal atomic ratio*. The penetration of the XPS beam concerns a thickness that does not exceed 2.5 nm. The surface S/Zr atomic ratio was almost the same in the nonpromoted and the Ga-promoted samples. For the samples containing the other promoters, this ratio was higher than those determined for the nonpromoted

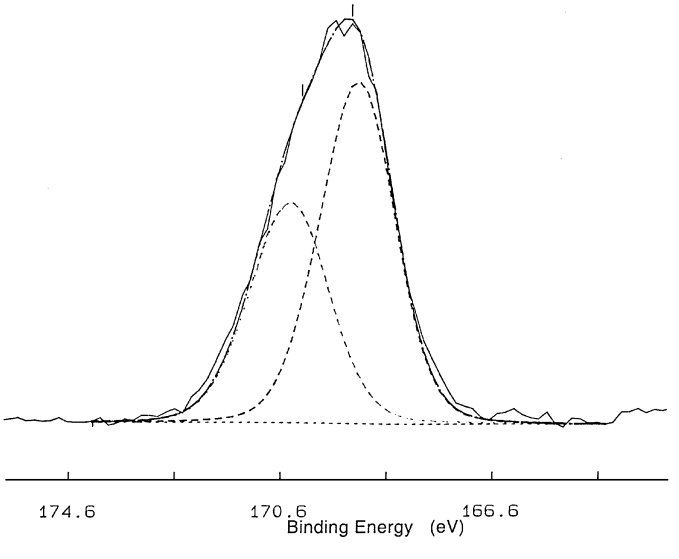

FIG. 11. Typical XPS spectra in the region of S 2*p*.

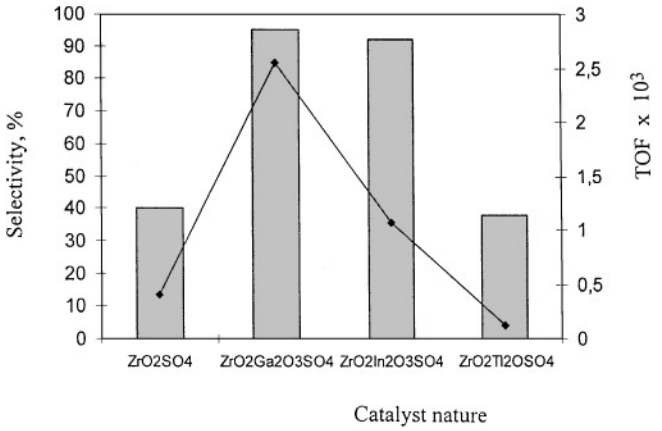

FIG. 12. Variation of the selectivity to methylcyclopentane (■) and of the TOF (◆) for the catalysts activated in Ar (T, 140°C; space velocity, 5.4 h^{-1}).

samples. However, the sulfur-to-total metal content ratio was lower than the sulfur-to-zirconium ratio in non-promoted samples, and this ratio decreased from the sample containing Ga to the one containing Tl. One should note that the sulfur-to-zirconium atomic ratios differ from those determined from the chemical analyses. Irrespective of the chemical composition, the value obtained from XPS measurements exceeded those established by chemical analysis. From these results, it could be concluded that, regardless of the chemical composition, sulfate groups are majoritary on the external surface.

3.4. Catalytic Tests

Dehydrocyclization of hexane was the main reaction occurring on the investigated catalysts. Figure 12 shows the variation of the TOF and of the selectivity to methylcyclopentane on the catalysts activated in Ar. Promotion with Ga and In enhanced the selectivity to methylcyclopentane compared with nonpromoted sulfated zirconia. The difference (100 − Sel.)% on Ga- and In-promoted catalysts mainly represents the cracked products (%). On nonpromoted and Tl-promoted sulfated zirconias, high yields of branched C_6 hydrocarbons were formed.

Figure 13 shows the variation of the dibranched-to-monobranched hydrocarbon ratio (a) and of the isomerized C_6 hydrocarbons-to-cyclic hydrocarbons ratio (b), respectively, as a function of conversion for both the catalysts activated in air and Ar. Air activation favours isomerization to dibranched hydrocarbons and depresses the dehydrocyclization activity.

It is worth noting that in the case of Ga, the reaction rate was about five times higher than for the nonpromoted catalyst. An increase of the reaction rate by about 2 was also determined for the In-promoted catalyst. Introduction of Tl had an opposite effect, namely a decrease of the reaction rate relative to sulfated zirconia (Table 3).

The activation energies given in Table 3 have small values indicating that adsorption is a determining step in the reaction. Experiments carried out on catalysts with different particle sizes showed no modification of the reaction rate, suggesting that the mass transfer processes are not responsible for this behavior. In addition, the values given in Table 3 were obtained at space velocities as high as 5.4 h^{-1}.

Figure 14 shows the variation of the selectivity and of the TOF when methylcyclopentane was used as reactant. The main reaction product was cyclohexane. The presence of In and Tl brought about a decrease of the isomerisation activity to cyclohexane and an enhancement of the ring cleavage activity, branched C_6 molecules being the dominant products. The cracking products were formed in lesser amounts

TABLE 3

Conversion of *n*-Hexane over Sulfated-Zirconium Catalysts

		Activated in Ar, 823 K							Activated in air, 823 K						
			Selectivity, mol%							Selectivity, mol%					
Sample	T (K)	TOF[a] ×10³	CH	MCP	C[b]	(d/m)[c]	B	E (kcal/mol)	TOF[a] ×10³	CH	MCP	C[b]	(d/m)[c]	B	E (kcal/mol)
$ZrO_2 \cdot SO_4^{2-}$	393	0.17	21.4	39.4	7.3	0.29	0.2	6.8	0.41	18.8	43.3	7.4	0.31	2.3	7.0
	513	1.30	19.6	38.4	8.8	0.31	0.3		3.30	12.5	41.8	9.0	0.34	2.9	
$ZrO_2 \cdot Ga_2O_3 \cdot SO_4^{2-}$	393	0.85	0.2	92.1	5.4	0.30	2.2	7.1	1.02	24.8	37.3	7.4	0.32	0.4	7.0
	513	7.17	0.1	89.7	7.3	0.31	2.8		8.24	22.5	35.8	9.0	0.34	0.6	
$ZrO_2 \cdot In_2O_3 \cdot SO_4^{2-}$	393	0.51	1.0	89.2	8.0	0.32	0.9	6.8	0.38	25.9	40.3	8.3	0.33	0.6	6.9
	513	3.93	0.9	87.6	9.1	0.34	1.4		1.40	23.2	38.9	9.4	0.35	0.9	
$ZrO_2 \cdot Tl_2O \cdot SO_4^{2-}$	393	0.07	14.1	38.3	7.6	0.29	—	8.9	0.31	16.80	39.9	5.0	0.23	—	9.4
	513	1.00	12.5	37.0	8.3	0.24	—		5.20	15.20	38.8	7.3	0.25	—	

Note. Data recorded after 5-min reaction. CH, cyclohexane; MCP, metylcyclopentane; B, benzene.

[a] $mol \cdot (mol\ SO_4^{2-})^{-1} \cdot s^{-1}$.

[b] Cracked products, i.e., hydrocarbons containing <number of carbon atoms lower than 6.

[c] The molar ratio of di- and monobranched hexane isomers.

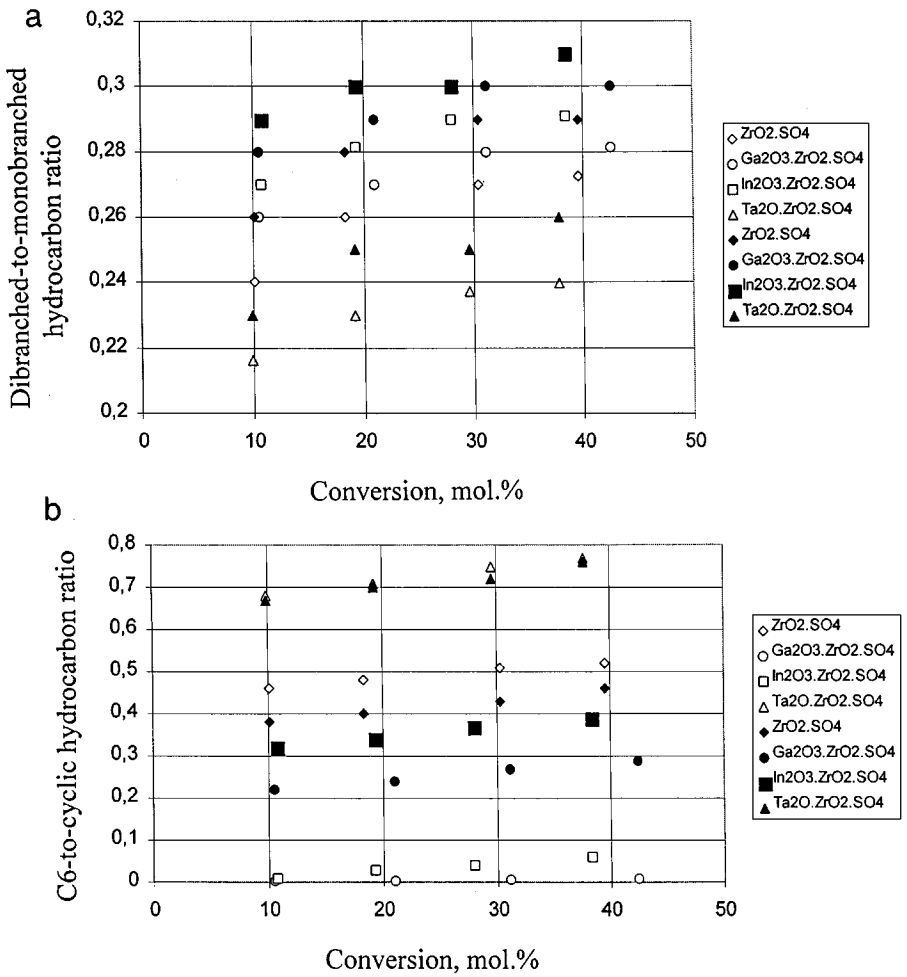

FIG. 13. Variation of the dibranched-to-monobranched hydrocarbon ratio (a) and of the isomerized C_6 hydrocarbons-to-cyclic hydrocarbon ratio (b) as a function of conversion for the catalysts activated both in Ar and air (T, 160°C; ◇, ○, □, △, catalysts activated in Ar; ◆, ●, ■, ▲, catalysts activated in air).

than in the reaction of hexane. At the same time, the reaction rate was one order of magnitude lower than those found for hexane. Again, the Ga-containing catalyst exhibited a high reaction rate while the Tl-promoted sample had the lowest value. The activity of the In-promoted catalyst was inferior to that of the pure sulfated zirconia. The activation energies were in the same range of values, also pointing to adsorption as the rate determining step (Table 4).

Figure 15 shows the variation of the dibranched-to-monobranched hydrocarbon ratio (a) and of the isomerized C_6 hydrocarbons-to-cyclohexane ratio (b), respectively, as a function of conversion for the catalysts activated both in air and Ar. As for hexane, air activation of the catalysts favours the isomerization to dibranched hydrocarbons. The increase of the conversion corresponds to a slight increase of ring opening. This is more evident for In- and Tl-promoted catalysts.

In the reaction of cyclohexane, cyclic products, namely methylcyclopentane, also predominated. A high selectivity

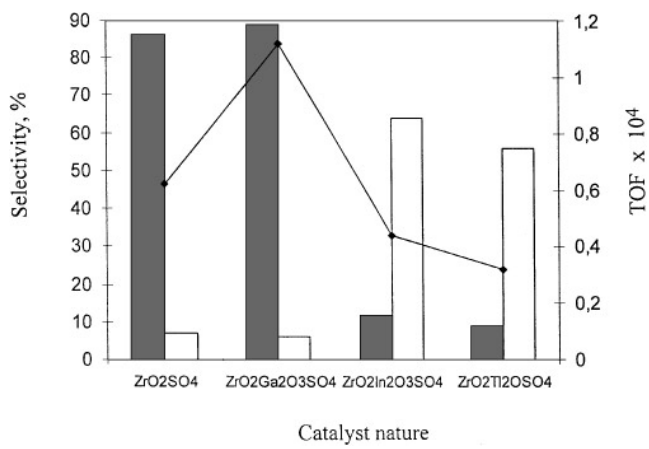

FIG. 14. Variation of the selectivity to cyclohexane (■) and branched C6 hydrocarbons (□), and of the TOF (◆) for the catalysts activated in Ar (T, 140°C; space velocity, 5.4 h^{-1}).

TABLE 4

Conversion of Metylcyclopentane over Sulfated-Zirconium Catalysts

Sample	T (K)	Activated in Ar, 823 K: TOF[a] $\times 10^4$	Selectivity, mol% CH	*n*-C6	C[b]	(d/m)[c]	E (kcal/mol)	Activated in air, 823 K: TOF[a] $\times 10^4$	Selectivity, mol% CH	*n*-C6	C[b]	(d/m)[c]	E (kcal/mol)
$ZrO_2 \cdot SO_4^{2-}$	393	0.50	85.2	1.2	1.7	0.28	6.3	0.61	87.4	1.9	2.2	0.31	6.5
	513	3.32	84.8	1.7	4.0	0.30		4.30	86.8	1.8	4.3	0.32	
$ZrO_2 \cdot Ga_2O_3 \cdot SO_4^{2-}$	393	1.08	88.4	2.6	0.7	0.20	6.5	1.48	89.9	4.2	1.1	0.21	6.7
	513	7.61	86.0	2.8	3.4	0.24		11.08	87.6	4.4	3.9	0.24	
$ZrO_2 \cdot In_2O_3 \cdot SO_4^{2-}$	393	0.37	10.2	4.3	1.6	0.26	6.8	0.51	11.8	5.1	1.9	0.28	7.2
	513	2.85	9.1	4.8	3.1	0.28		4.44	10.6	5.1	3.5	0.29	
$ZrO_2 \cdot Tl_2O \cdot SO_4^{2-}$	393	0.26	8.1	3.4	1.9	0.31	7.1	0.41	9.1	3.9	2.6	0.32	7.4
	513	0.78	6.4	3.7	4.3	0.32		3.79	7.9	3.7	4.7	0.34	

Note. Data recorded after 5-min reaction. CH, cyclohexane; *n*-C6, the sum of *n*-hexane and *n*-hexene.
[a] $mol \cdot (mol\ SO_4^{2-})^{-1} \cdot s^{-1}$.
[b] Cracked products, i.e., hydrocarbons containing a number of carbon atoms lower than 6.
[c] The molar ratio of di- and monobranched hexane isomers.

to methylcyclopentane was again achieved on the Ga-promoted catalyst (Fig. 16). However, even with In and Tl, these compounds were predominant. The dependence of the reaction rate on the catalyst nature showed the same features as those observed for methylcyclopentane, but the values were slightly smaller (Table 5). A similar behavior is also noticed from the dependence of the selectivity on the conversion (Fig. 17). Again the increase of the conversion is accompanied by a slight increase of the noncyclic hydrocarbons.

DISCUSSION

The characterization of the samples with the different techniques indicates that the main factors which control the observed properties are the high sulfur content and the promoter effect. It has been shown in the literature that the development of the acid sites in these catalysts requires an amorphous structure of zirconia (53–56). Such materials are easily synthesised by the sol–gel method and, in particular, by the colloidal sol–gel approach, which is a variant of the sol–gel route. In addition, this method allows us to achieve a homogeneous distribution of the components, in the occurrence of the promoters.

Generally, the surface area of sulfated zirconia obtained via the one-step sol–gel polymeric method exceeds 120 $m^2\ g^{-1}$. In the case of the colloidal sol–gel route, lower surface areas are consistent with sulfur content as high as 14 wt% SO_4^{2-}. But this behavior also needs to be related to the preparation procedure. Tichit *et al.* (57) obtained

TABLE 5

Conversion of Cyclohexane over Sulfated-Zirconia Catalysts

Sample	T (K)	Activated in Ar, 823 K: TOF[a] $\times 10^4$	Selectivity, mol% MCP	*n*-C6	C[b]	(d/m)[c]	E (kcal/mol)	Activated in air, 823 K: TOF[a] $\times 10^4$	Selectivity, mol% MCP	*n*-C6	C[b]	(d/m)[c]	E (kcal/mol)
$ZrO_2 \cdot SO_4^{2-}$	393	0.13	50.9	6.0	4.9	0.29	7.4	0.19	58.8	6.0	5.0	0.30	8.1
	513	1.20	48.1	6.4	6.8	0.30		2.10	54.1	6.3	8.4	0.32	
$ZrO_2 \cdot Ga_2O_3 \cdot SO_4^{2-}$	393	0.36	70.9	2.2	3.8	0.26	7.3	0.40	74.4	1.9	4.4	0.27	7.8
	513	3.23	68.4	2.4	6.6	0.27		4.18	70.9	2.2	7.3	0.29	
$ZrO_2 \cdot In_2O_3 \cdot SO_4^{2-}$	393	0.09	51.2	6.0	6.6	0.29	7.4	0.14	54.0	5.8	5.4	0.31	8.4
	513	1.06	47.7	6.4	8.8	0.30		1.75	49.2	7.1	9.6	0.34	
$ZrO_2 \cdot Tl_2O \cdot SO_4^{2-}$	393	0.07	38.3	3.2	3.6	0.20	8.5	0.19	40.1	5.2	3.7	0.19	8.7
	513	0.90	36.6	6.6	6.6	0.23		0.95	39.0	5.5	7.1	0.22	

Note. Data recorded after 5-min reaction. MCP, methylcyclopentane; *n*-C6, the sum of *n*-hexane and *n*-hexene.
[a] $mol \cdot (mol\ SO_4^{2-})^{-1} \cdot s^{-1}$.
[b] Cracked products, i.e., hydrocarbons containing a number of carbon atoms lower than 6.
[c] The molar ratio of di- to monobranched hexane isomers.

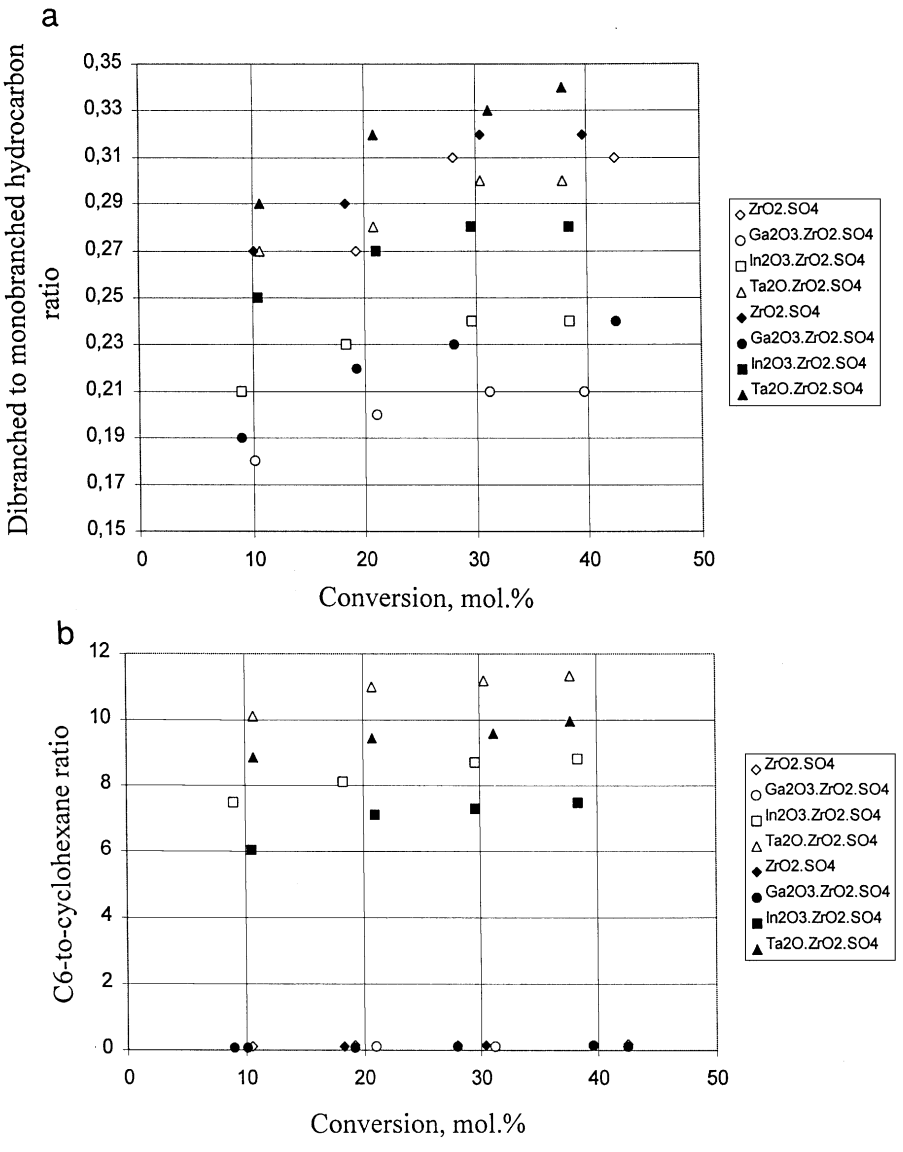

FIG. 15. Variation of the dibranched-to-monobranched hydrocarbon ratio (a) and of the isomerized C_6 hydrocarbons-to-cyclohexane ratio (b) as a function of conversion for the catalysts activated both in Ar and air (T, 160°C; ◇, ○, □, △, catalysts activated in Ar; ◆, ●, ■, ▲, catalysts activated in air).

catalysts with similar sulfur content (about 16 wt% SO_4^{2-}) by impregnation of high surface area zirconia with H_2SO_4 in which zirconia keeps its texture. Low-surface-area catalysts were also obtained by Fårcasiu and Li (33) using a percolation method. In our case, the rather low surface areas and the high sulfur-to-zirconium ratios obtained by XPS compared with the values established by chemical analysis led us to suppose that sulfate species primarily form some polymeric superficial sites. Moreover, if one compares the density of the SO_4^{2-} groups per nm^2, values as high as 10 compared with 2–2.5 determined by Bensitel *et al.* (50) and Morterra *et al.* (42) appear to be unusual. Therefore, one may assume that part of the sulfate in these catalysts exists as sulfuric acid supported on these materials, which could also account for the quasi-absence of micropores. Summarizing, the solids prepared via the colloidal sol–gel method have a mesoporous texture in which part of the sulfate is as supported sulfuric acid which may possibly fill or block the micropores. The shape of the adsorption–desorption isotherms corresponds to type III solids, except for the Tl-containing sample activated in Ar, which exhibits type II hysteresis.

Before calcination, the solids are X-ray amorphous, regardless of the sulfur content. Calcination at 550°C induces the structuration of these materials and the X-ray patterns show peaks corresponding to two different zirconium sulfates as well as to zirconium oxides. This means that even in conditions of sol–gel preparation, a perfectly homogeneous

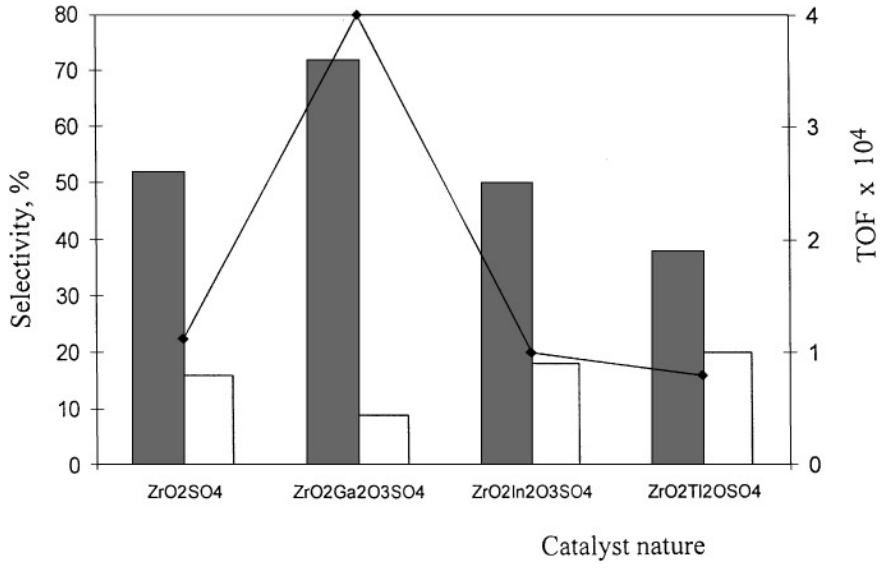

FIG. 16. Variation of the selectivity to methylcyclopentane (■) and branched C6 hydrocarbons (□), and of the TOF (◆) for the catalysts activated in Ar (T, 140°C; space velocity, 5.4 h^{-1}).

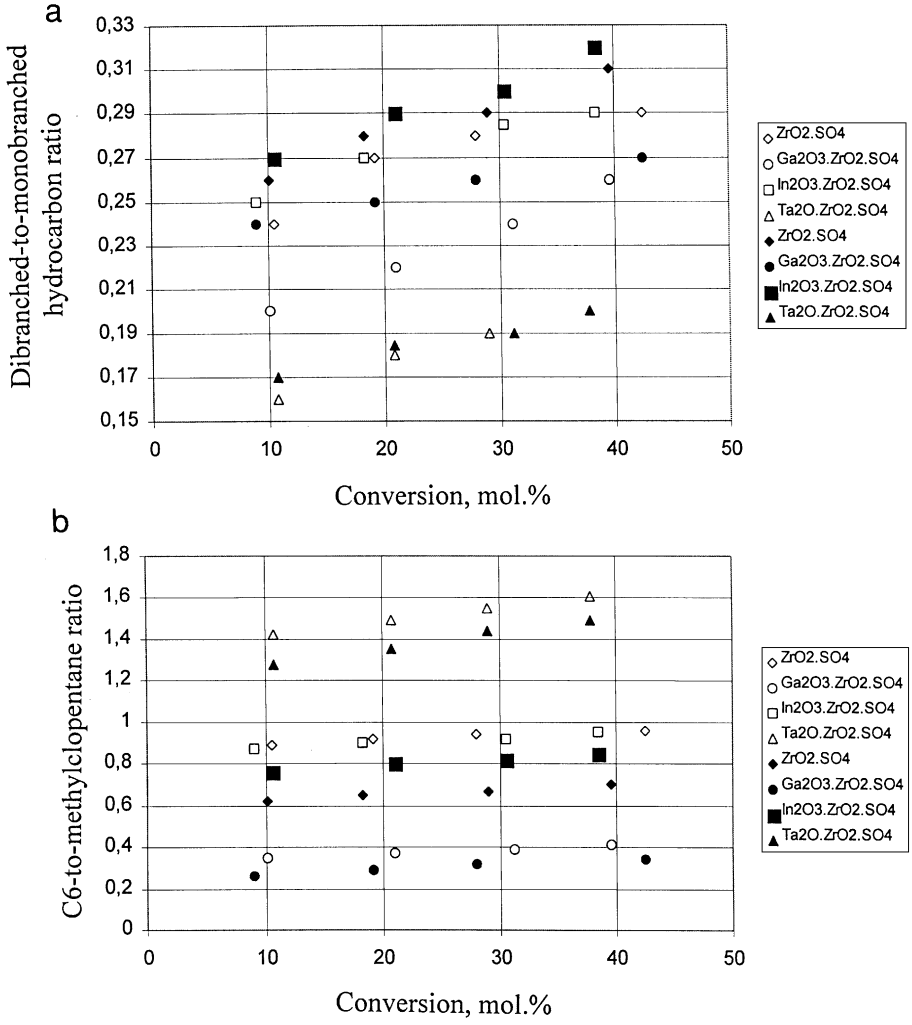

FIG. 17. Variation of the dibranched-to-monobranched hydrocarbon ratio (a) and of the isomerized C_6 hydrocarbons-to-methylcyclopentane ratio (b) as a function of conversion for the catalysts activated both in Ar and air (T, 160°C; ◇, ○, □, △, catalysts activated in Ar; ◆, ●, ■, ▲, catalysts activated in air).

structure is far from being achieved. No lines corresponding to Ga, In, or Tl species were noticed but, instead, reflections due to an unidentified phase (? in Figs. 7 and 8) were detected.

Raman spectroscopy provided additional information on the nature of the sulfate species. Bands attributable to S-O and S=O stretching modes of sulfate groups in different coordination (40, 46–48) were observed: isolated sulfate groups, polynuclear sulfate species, and sulfuric acid (Figs. 5 and 6). The last two species were clearly identified. In addition, the band attributed to polynuclear species contains more than one component, which presumably indicates the existence of different polynuclear species with different polymerization degrees.

Acidity is the most important function of sulfated zirconia and it is evidently related to the presence of SO_4 groups. Indeed, zirconium oxides exhibit only weak acidic properties, irrespective of their synthesis method (58). Structural characterizations indicate a very heterogeneous surface: isolated and polymeric sulfate species as well as zirconium oxide being equally accessible. In addition, supported sulfuric acid is also very probably present.

FTIR spectra of adsorbed bases showed the presence of both Brønsted and Lewis sites, whatever the catalyst composition. The presence of promoters brought about a decrease of the population of polynuclear sulfates, in the sequence Tl > In > Ga. Also, the amount of Brønsted acid sites was lowered in the promoted samples.

The nature of the Brønsted acidity in these catalysts is still a debated question. Knözinger and co-workers (46, 47) and Kustov *et al.* (59) attribute the Brønsted acidity to isolated monosulfate species, while Morterra *et al.* (42, 60) and Platero *et al.* (41) consider that these sites should be associated with disulfate species. These different authors, however, agree on the role of residual water in determining the Brønsted acidity. In our catalysts, the Brønsted sites could be due to "hydrated" polynuclear species but also to supported sulfuric acid. In addition, the water which generates the Brønsted acidity could be held in the system by the same supported species. These results when related with those obtained from Raman spectroscopy allow us to speculate that, in these catalysts, Lewis acidity results, as generally outlined in the literature, from the inductive effect exerted by strongly bonded sulfate groups (mono- or polynuclear species). As a consequence, the model for the acid sites in such a case is quite complicated.

The atmosphere in which the catalysts were activated was found to influence both the density and, to a lesser extent, the strength of the acid sites. Activation in air provoked a slight decrease of the sulfur content. This decrease is concomitant with a slight diminution of the surface area and with an increase of the acid strength. Therefore, it may assumed that the presence of air favours the nucleation of the superficial sulfate groups. During this process, a small part of the sulfate is eliminated. In all the cases, a temperature of 550°C was found to determine the strong acidic properties.

It emerges from the literature that the transformation of linear (29, 57, 61) and cyclic (62, 63) C_6 hydrocarbons requires strong acid sites. In this study, hexane, methylcyclopentane, and cyclohexane were converted over the different catalysts investigated. These results are in agreement with numerous published works which underline the strong acid character of sulfated zirconias, in spite of differences in the activities according to the hydrocarbon and the catalyst promoter. Also, the aromatization function of Ga introduced in ZSM-5 zeolites has been stressed in the literature. The catalytic functions responsible for the activity of (Ga, H)-ZSM-5 or (In, H)-ZSM-5 as dehydrocyclization (aromatization) catalysts are acidity and redox properties of Ga or In. The oxidation state of these elements can cycle between +3 and +1 during reaction, whereas Tl^+ cannot. The results obtained will be discussed with respect to the nature of the hydrocarbon.

(a) Hexane

The analysis of the reaction products indicates that on the non-promoted and the Tl-promoted catalysts, hexane was transformed according to three different reactions: chain isomerization, cyclization, and cracking. On Ga- and In-promoted sulfated zirconias, only cyclization and cracking reactions were evidenced. These reactions require the presence of acid sites but with different strengths. In addition, except for the Tl-promoted catalysts, small amounts of benzene were also detected.

It is now accepted that the first step in the isomerization reaction on these catalysts is the dehydrogenation of the hydrocarbon. The hydroisomerization mechanism suggested can be divided in (de)hydrogenation, protonation, and isomerization steps (64). A bifunctionality in the isomerization of pentane was also reported by Salmones *et al.* (65). In our case, the disappearence of the Raman bands corresponding to deprotonated sulfate species and the increase of the intensity of the bands corresponding to protonated species also support this mechanism. The modification of the XPS-S 2p (169 eV) to the S 2p (170 eV) signal ratio is consistent with the same process. The role of dehydrogenation has also been clearly proved by Ghenciu and Fårcasiu (66) and Srinivasan *et al.* (8) using benzene as a probe molecule. They explained this process as a one-electron oxidation of the alkane, which implies the oxidation ability but does not require superacidity. The first step is a slow one and the initiation time, also observed by Lonyi *et al.* (22) and Fårcasiu *et al.* (34), could correspond to the dehydrogenation step.

The formation of polyenic cation species which may be assumed from the Raman band located at 433 cm^{-1} is another argument in favor of this process. Alkylsulfates

have been proposed as intermediates by Kazansky (67) and Cheng and Ponec (68).

The importance of calcination and the necessity for Lewis acid sites in the reaction of aliphatic hydrocarbons on sulfated zirconias have been intensely discussed in the literature. Most of the Lewis sites are generated during calcination, and their presence appears to be very important to the first dehydrogenation step.

Low activation energies were found to be the consequence of the strong adsorption of the reactants and reaction intermediates, which would be the determining step in this reaction. A similar conclusion has been previously drawn by Adeeva *et al.* (45) who stressed that "the extraordinary activity of these catalysts is likely to be caused by a good stabilization of the surface intermediates."

But the strong adsorption also causes a rapid deactivation of the catalysts. Raman spectra showed that after reaction, and concomitant with the strong increase of the protonated sulfate species on the catalysts surface, bands due to organic species appear. The mechanism through which this process occurs is probably similar to the one proposed by Signoretto *et al.* (69). Bands assigned to polyenic and aromatic species were found in the Raman spectra of the samples exposed to hexane vapour. Small amounts of benzene were also found among the reaction products. Knözinger and co-workers (46, 47) proved that these species contribute to the catalyst's deactivation.

Another cause of deactivation could result from a partial loss of sulfur. XPS data showed that after reaction, the S/Zr atomic ratio was significantly lower in the case of the catalysts with high sulfur content than before reaction. For catalysts containing less sulfur, this decrease was not as important. Similar conclusions were drawn very recently by Vaudagna *et al.* (36).

The differences observed between the catalysts activated in argon and in air could be accounted for by the fact that for the latter ones, more deprotonated and dimeric species exist.

(b) Methylcyclopentane

Except for the Ga-promoted catalyst, methylcyclopentane has also been found to react differently on the investigated catalysts, namely, via three routes: isomerization (first to cyclohexane), ring opening (possibly accomplished by a second isomerization process to mono- and dibranched molecules), and cracking. Again, on the Ga-promoted catalyst, only ring isomerization and cracking were evidenced. On those catalysts and in our experimental conditions, activation of methylcyclopentane is more difficult and this could explain the low conversions (compared with those obtained for hexane) and reaction rates, and the low cracking contents in the reaction products.

Dehydrogenation occurs to a small extent and only on nonpromoted and Ga-promoted catalysts, which may be accounted for from the Raman and XPS results. Indeed, the Raman spectra recorded after exposure of the samples to methylcyclopentane still showed bands attributable to unprotonated sulfate groups, and the intensity of the band attributed to polyenic species was much reduced. Besides, no band related to C=C stretching vibrations of compounds with an increased aromatic character (at about 1517 cm^{-1}) was observed.

The XPS ratio of the S 2p components at 169 and 170 eV was closer to the values recorded on fresh catalysts than to those of samples exposed to hexane. The XPS sulfur content of the samples exposed to methylcyclopentane was also higher than those determined in the case of hexane.

The very low activation energies again point to the fact that the determing step is not the reaction but the adsorption. The activation energies were determined from the TOF dependence on temperature. The values reported by Fårcasiu *et al.* (34) are more rigorous because they distinguished isomerization and deactivation. However, at the temperatures at which the reactions were carried out, the activation energies should be lower.

(c) Cyclohexane

The reaction of cyclohexane was intermediate between hexane and methylcyclopentane. Cyclohexane reacted following the similar routes as methylcyclopentane: isomerization, ring opening, and cracking. The reactivities were found to be slightly smaller than for methylcyclopentane. Methylcyclopentane was the dominant reaction product, irrespective of the catalyst nature and reaction conditions, which allows us to suppose that on these catalysts, these reactions are reversible. The higher activation energies compared with those determined in the case of hexane or methylcyclopentane indicate that adsorption probably plays a less important contribution.

CONCLUSION

Sulfatation of zirconium hydroxide requires an amorphous reactive precursor. Both sulfated zirconia and Ga-, In-, or Tl-promoted sulfated zirconias correspond to such solids. A sulfate concentration as high as 50 wt% determines a particular texture of these materials characterized by a pore diameter in the mesoporous range. The sulfate groups in these catalysts are in different coordinations: isolated species, polynucleated species, and supported acid. As a consequence, both Lewis and Brønsted acid sites with different strengths coexist. The amount of water necessary to promote Brønsted acidity could correspond to that retained by supported H_2SO_4. Activation in air was found to "catalyze" the formation of the polynucleate species and, as a consequence, to increase the acid strength. Promotion resulted in an increase of the Lewis acid sites population in the order Ga > In > Tl.

Catalytic tests carried out in the presence of C6 saturated hydrocarbons showed different reactivities according to the nature of the hydrocarbon and of the promoter. The first step of the reaction implies the abstraction of at least one hydrogen atom and, for this process, Lewis acid sites are those mainly responsible. Hydrogen was not detected in the reaction products but instead, Raman spectra showed a large contribution of the protonated species after the samples were exposed to a hydrocarbon flow.

Hydrogen abstraction is the cause of the activity of these catalysts, but also of their deactivation. More dehydrogenated species lead to polymerization. At the same time, the abstraction capacity of the catalysts is limited by the sulfur content. Samples containing more sulfate allow a more advanced dehydrogenation and, as a consequence, cyclisation of C_6 hydrocarbons. XPS data confirmed the existence of redox processes and, in addition, they showed that a partial removal of sulfur occurs during these processes.

The presence of Ga seems to enhance the dehydrogenation activity, but it is not clear yet whether this is due to the increase of the Lewis sites population or to their participation as redox sites.

REFERENCES

1. Holm, V. C. F., and Bailey, G. C., U.S. Patent 3,032,599 (1962).
2. Tanabe, K., Itoh, M., Morishiga, K., and Hattori, H., *in* "Studies in Surface Science and Catalysis," Vol. 1, p. 65. Elsevier, Amsterdam, 1976.
3. Hino, M., and Arata, K., *J. Chem. Soc. Chem. Commun.* 1148 (1979).
4. Hino, M., and Arata, K., *Chem. Lett.* 1259 (1979).
5. Jin, T., Machida, M., Yamaguchi, T., and Tanabe, K., *Inorg. Chem.* **23**, 4396 (1984).
6. Yang, T.-S., Chang, T.-H., and Yeh, C.-T., *J. Mol. Catal. A Chem.* **115**, 339 (1997).
7. Bazin, P., Saur, O., Lavalley, J. C., Blanchard, G., Visciglio, V., and Touret, O., *Appl. Catal. B Envir.* **13**, 265 (1997).
8. Srinivasan, R., Keogh, R. A., Ghenciu, A., Fårcasiu, D., and Davis, B. H., *J. Catal.* **158**, 502 (1996).
9. Brunner, E., *Catal. Today* **38**, 361 (1997).
10. Hollstein, E. J., Wie, J. T., and Hsu, C.-Y., U.S. Patent 4,918,041 (1990).
11. Hollstein, E. J., Wie, J. T., and Hsu, C.-Y., U.S. Patent 4,956,519 (1990).
12. Lin, C.-H., and Hsu, C. -Y., *J. Chem. Soc. Chem. Commun.* 1497 (1992).
13. Hsu, C.-Y., Heimbuch, C. R., Armes, C. T., and Gates, B. C., *J. Chem. Soc. Chem. Commun.* 1645 (1992).
14. Cheung, T.-K., d'Itri, J. L., and Gates, B. C., *J. Catal.* **151**, 464 (1995).
15. Cheung, T.-K., Lange, F. C., and Gates, B. C., *J. Catal.* **159**, 99 (1996).
16. Jatia, A., Chang, C., MacLeod, J. D., Okubo, T., and Davis, M. E., *J. Catal.* **152**, 21 (1994).
17. Wan, K. T., Khouw, C. B., and Davis, M. E., *J. Catal.* **158**, 311 (1996).
18. Ghenciu, A., and Fårcasiu, D., *Catal. Lett.* **44**, 29 (1997).
19. Sikabwe, E. C., and White, R. L., *Catal. Lett.* **44**, 177 (1997).
20. Alvarez, W. E., Liu, H., and Resasco, D. E., *Appl. Catal. A Gen.* **162**, 103 (1997).
21. Vera, C. R., Yori, J. C., and Parrera, J. M., *Appl. Catal. A Gen.* **167**, 75 (1998).
22. Lonyi, F., Valyon, J., Engelhardt, J., and Mizukami, F., *J. Catal.* **160**, 279 (1996).
23. Xu, B.-Q., and Sachtler, W. M. H., *J. Catal.* **165**, 231 (1997).
24. Iglesia, E., Soled, S. L., and Kramer, G. M., *J. Catal.* **144**, 238 (1993).
25. Soled, S. L., Iglesia, E., and Kramer, G. M., *in* "Studies in Surface Science and Catalysis," Vol. 90, p. 531. Elsevier, Amsterdam, 1994.
26. Price, C. L., and Kanazirev, V., *J. Catal.* **126**, 267 (1990).
27. Iglesia, E., Baumgarten, J. E., and Price, C. L., *J. Catal.* **134**, 549 (1992).
28. Guisnet, M., Gnep, N. S., and Alario, F., *Appl. Catal.* **89**, 1 (1992).
29. Ono, Y., *Catal. Rev. Sci. Eng.* **34**, 179 (1992).
30. Granetto, G., Monque, R., and Galliasso, R., *Catal. Rev. Sci. Eng.* **36**, 271 (1994).
31. Choudhary, V. R., Devadas, P., Kinaga, A. K., and Guisnet, M., *J. Catal.* **158**, 125 (1996).
32. Pârvulescu, V. I., Frunza, L., Catana, G., Russu, R., and Pârvulescu, V., *Appl. Catal. A Gen.* **121**, 69 (1995).
33. Fårcasiu, D., and Li, J. Q., *Appl. Catal. A Gen.* **128**, 97 (1995).
34. Fårcasiu, D., Li, J. Q., and Kogelbauer, A., *J. Mol. Catal. A Chem.* **124**, 67 (1997).
35. Comelli, R. A., Finelli, Z. R., Vaudagna, S. R., and Figoli, N. S., *Catal. Lett.* **45**, 227 (1997).
36. Vaudagna, S. R., Comelli, R. A., and Figoli, N. S., *Catal. Lett.* **47**, 259 (1997).
37. Sing, K. S. W., and Rouquerol, J., *in* "Handbook of Heterogeneous Catalysis" (G. Ertl, H. Knözinger, and J. Weitkamp, Eds.), Vol. 2, p. 427. Wiley-VCH, Berlin, 1997.
38. Nakano, Y., Iizuka, T., Hattori, H., and Tanabe, K., *J. Catal.* **57**, 1 (1979).
39. Waquif, M., Bachelier, J., Saur, O., and Lavalley, J. C., *J. Mol. Catal.* **72**, 127 (1992).
40. Babou, F., Coudurier, G., and Vedrine, J. C., *J. Catal.* **152**, 341 (1995).
41. Platero, E. E., Mentruit, M. P., Arean, C. O., and Zecchina, A., *J. Catal.* **162**, 268 (1996).
42. Morterra, C., Cerrato, G., Emanuel, C., and Bolis, V., *J. Catal.* **142**, 349 (1993).
43. Nascimento, P., Akratopoulou, C., Oszgyan, M., Coudurier, G., Travers, C., Joly, J. F., and Vedrine, J. C., *in* "Proceedings, 10th International Congress on Catalysis, Budapest, 1992" (L. Guczi, F. Solymosi, and P. Tetenyi, Eds.), Vol. 1, p. 1185. Akadémiai Kiadó, Budapest, 1993.
44. Pelmeschikov, A. G., van Santen, R. A., Jänchen, J., and Meijer, E., *J. Phys. Chem.* **97**, 1071 (1993).
45. Adeeva, V., de Haan, J. V., Jänchen, J., Lei, G. D., Schünemann, V., van de Ven, L. J. M., Sachtler, W. M. H., and van Santen, R. A., *J. Catal.* **151**, 364 (1995).
46. Riemer, T., Spielbauer, D., Hunger, M., Mekhemer, G. A. H., and Knözinger, H., *J. Chem. Soc. Chem. Commun.* 1181 (1994).
47. Spielbauer, D., Mekhemer, G. A. H., Bosch, E., and Knözinger, H., *Catal. Lett.* **36**, 59 (1996).
48. Li, C., and Stair, P. C., *Catal. Lett.* **36**, 119 (1996).
49. Babou, F., Bigot, B., Coudurier, G., Sautet, P., and Vedrine, J. C., *in* "Studies in Surface Science and Catalysis," Vol. 90, p. 519. Elsevier, Amsterdam, 1994.
50. Bensitel, M., Saur, C., Lavalley, J. C., and Morrow, B. A., *Mater. Chem. Phys.* **19**, 147 (1988).
51. Morterra, C., Cerrato, G., and Bolis, V., *Catal. Today* **17**, 505 (1993).
52. Fraenkel, D., *Ind. Eng. Chem. Res.* **36**, 52 (1997).
53. Chen, F. R., Coudurier, G., Joly, J. F., and Vedrine, J. C., *J. Catal.* **143**, 616 (1993).
54. Ward, D. A., and Ko, E. I., *J. Catal.* **157**, 321 (1995).
55. Ward, D. A., and Ko, E. I., *Ind. Eng. Chem. Res.* **34**, 425 (1995).
56. Morterra, C., Cerrato, G., Pinna, F., Signoretto, M., and Strukul, G., *J. Catal.* **149**, 181 (1994).
57. Tichit, D., El Alami, D., and Figueras, F., *J. Catal.* **163**, 18 (1996).
58. Tanabe, K., Misono, M., and Ono, Y., *in* "Studies in Surface Science and Catalysis," Vol. 51, p. 1909. Elsevier, Amsterdam, 1989.

59. Kustov, L. M., Kazansky, V. B., Figueras, F., and Tichit, D., *J. Catal.* **150**, 143 (1994).
60. Morterra, C., Bolis, V., Cerrato, G., and Magnacca, G., *Surf. Sci.* **307**/**309**, 1206 (1994).
61. Ebitani, K., Tsuji, J., Hattori, H., and Kita, H., *J. Catal.* **135**, 609 (1992).
62. de la Puente, G., and Sedran, U., *Appl. Catal. A Gen.* **144**, 147 (1996).
63. Corma, A., Mocholi, F., Orchilles, V., Koermer, G. S., and Maden, R. J., *Appl. Catal.* **67**, 307 (1991).
64. van de Runstraat, A., Kamp, J. A., Stobbelaar, P. J., van Grondelle, J., Krijnen, S., and van Santen, R. A., *J. Catal.* **171**, 77 (1997).
65. Salmones, J., Licona, R., Navarrete, J., Salas, P., and Morales, J., *Catal. Lett.* **36**, 135 (1996).
66. Ghenciu, A., and Fårcasiu, D., *J. Mol. Catal. A Chem*. **109**, 273 (1996).
67. Kazansky, V. B., *Acc. Chem. Res.* **24**, 379 (1991).
68. Cheng, Z. X., and Ponec, V., *Catal. Lett.* **25**, 337 (1994).
69. Signoretto, M., Pinna, F., Strukul, G., Chies, P., Cerrato, G., Di Ciero, S., and Morterra, C., *J. Catal.* **167**, 522 (1997).